JOURNAL OF MATERIALS SCIENCE **34** (1999) 2553–2560

Thermoplastic elastomers based on ionomeric polyblends of zinc salts of poly(propylene-co-acrylic acid) and carboxylated nitrile rubber

P. ANTONY, S. BANDYOPADHYAY, S. K. DE*
Rubber Technology Centre, Indian Institute of Technology, Kharagpur 721 302, India
E-mail: skde@rtc.iitkgp.ernet.in

Ionomeric polyblends of zinc salt of carboxylated nitrile rubber, abbreviated as Zn-XNBR and zinc salt of poly(propylene-co-acrylic acid), abbreviated as Zn-PPA, were prepared by melt blending. The ionomeric polyblends of Zn-XNBR/Zn-PPA in the compositions of 90/10 and 80/20, parts by weight, behave as ionic thermoplastic elastomers and exhibit synergism in properties. The ionomeric polyblend shows superior physical properties than the corresponding non-ionomeric polyblend. The synergism and superior physical properties of the ionomeric polyblends are attributed to the formation of strong intermolecular ionic interactions between the component polymers, as observed by the infrared spectroscopic studies. Dynamic mechanical thermal analyses reveal that besides glass-rubber transition in the low temperature region, the neat ionomers and the ionomeric polyblends show a high temperature transition owing to the relaxation of the restricted mobility chain segments in the ionic cluster region. The reprocessability studies reveal the thermoplastic elastomeric nature of the ionomeric polyblend.

1. Introduction

The introduction of ionic functional groups to modify the physical and mechanical properties of polymers have received wide attention [1–5]. This class of polymers, called ionomers, exhibit greater physical properties and melt viscosities than the corresponding non-ionic polymers, which is due to the interchain associations of the ionic groups [2–4]. The strong intermolecular associations between the ionic groups lead to microphase separated ion-rich domains, often called ionic clusters, which show a high temperature relaxation process in the viscoelastic behaviour [3, 4].

Besides improving the physical properties of the polymers, the ionic groups can improve the compatibility in the polyblends, wherein intermolecular ionic interactions facilitate the compatibilization [6, 7]. The mechanical properties of the polyblends are dependent on the interfacial adhesion between the two component phases and the specific interactions between the polymers are reported to promote the interfacial adhesion [8, 9]. There are several reports on compatible blends involving ion-ion and ion-dipole interactions [10–18]. Recently, De and coworkers have developed ionic thermoplastic elastomers from ionomeric polyblends [19–23].

The important objective of this paper aims at the development of an ionic thermoplastic elastomer from ionomeric polyblends of zinc oxide neutralized carboxylated nitrile rubber, abbreviated as Zn-XNBR and zinc oxide neutralized poly(propylene-co-acrylic acid), abbreviated as Zn-PPA.

2. Experimental

Details of the material used are given in Table I.

2.1. Preparation of ionomeric polyblends based on XNBR and PPA

Formulations used for the blend preparation are given in Table II. Ionomeric polyblends based on XNBR and PPA were prepared in a Brabender Plasticorder, model PLE-330 at 190 °C and at a rotor speed of 60 rpm. First PPA was allowed to melt for 5 min. Then XNBR was added and mixed for 2 min. Finally, zinc oxide and stearic acid were added and mixed for another 2 min. Preliminary studies showed that 10 phr of ZnO was sufficient for the neutralization of the carboxylic acid groups present in the polymers and 1 phr of stearic acid was found to increase the rate and extent of neutralization [24]. Stearic acid reacts with zinc oxide and produces zinc stearate, which increases the solubility of zinc oxide in the polymer matrix. After mixing the hot material was sheeted out in a two-roll mill. The blends were then moulded at 200 °C for 20 min in an electrically heated hydraulic press at a pressure

* Author to whom all correspondence should be addressed.

TABLE I Details of the materials used

Materials	Properties	Source
Carboxylated nitrile rubber, abbreviated as, XNBR	Grade X48/1 Acrylonitrile content, 29% Carboxylic monomer, 1% Mooney viscosity $ML_{(1+4)}$ at 100 °C, 40	Goodyear Rubber and Tyre Co., Akron, USA
Poly(propylene-co-acrylic acid), abbreviated as PPA (trade name, polybond 1002)	Acrylic acid content, 6% Molecular weight, (Mw) 240,000 Melt flow rate at 230 °C, 20 g/10 min	Uniroyal Chemical Co., USA
Zinc oxide	Rubber grade, Specific gravity, 5.6	E. Merck Ltd., Mumbai, India
Stearic acid	Rubber grade, Melting point, 76 °C	Obtained locally

TABLE II Formulations of the blends

	Blend number							
Ingredients	B0	B1	B2	B3	B4	B5	B6	B7
XNBR	100	90	80	70	60	50	0	80
PPA	0	10	20	30	40	50	100	20
ZnO	10	10	10	10	10	10	10	0
Stearic acid	1	1	1	1	1	1	1	0

of 5 MPa. After moulding was over the blends were cooled to room temperature by the circulation of cold water through the platens.

2.2. Measurement of physical properties

The stress-strain properties were measured with dumbbell samples according to ASTM D412 (1987) in a Zwick Universal Testing Machine (UTM), model 1445, at a crosshead speed of 500 mm/min. Tear strength was also measured in a Zwick UTM, model 1445, using 90° nick-cut crescent samples according to ASTM D624 (1986). The hardness was determined as per ASTM D2240 (1986) and expressed in Shore A units. The tension set at 100% extension was determined as per ASTM D412 (1987).

2.3. Infrared spectroscopic studies

Infrared spectroscopic studies on the compression moulded thin films of the samples were carried out using Perkin-Elmer 843 spectrophotometer, with a resolution of 3.2 cm^{-1}.

2.4. Dynamic mechanical thermal analysis

Dynamic mechanical thermal analyses were carried out in a Dynamic Mechanical Thermal Analyser (DMTA model No. MK-II, Polymer Laboratory, UK). The testing was performed in bending mode with a frequency of 3 Hz over a temperature range of −50 °C to 150 °C and at a heating rate of 2 °C/min.

2.5. Processability studies

The processability studies were carried out using Monsanto Processability Tester (MPT), model 83077, at the shear rates of 7.7, 15.4, 30.8 and 61.6 s^{-1} and at a temperature of 230 °C. The capillary length (32 mm) to diameter (2 mm) ratio (L/D) was 16. The preheat time for each sample was 5 min.

2.6. X-ray studies

X-ray studies of the samples were performed with Philips X-ray diffractometer (type PW-1840) using a nickel filtered CuK_α radiation from Philips X-ray generator (type PW-1729). Accelerating voltage and electric current were 40 kV and 20 mA respectively.

2.7. Scanning electron microscopic studies

Scanning electron micrographs of the tear fractured and cryogenically fractured blends were taken with scanning electron microscope (Hitachi, model S-415A, Japan). Accelerating voltage was 15 kV. The magnification of the samples were X300 and X500.

2.8. Reprocessability studies

The reprocessability studies of the 80/20, Zn-XNBR/Zn-PPA blend (blend B2) was studied by melting the moulded sample in the Brabender Plasticorder for 6 min at 190 °C and at a rotor speed of 60 rpm. The sample was then remoulded in the electrically heated hydraulic press for 20 min at 200 °C. The process of melting and moulding was repeated upto 3 cycles.

3. Results and discussion

3.1. Physical properties

The physical properties of the neat ionomers and the ionomeric polyblends are given in Table III. Fig. 1 shows the variation of tensile strength, tear strength and hardness with blend composition. It is apparent that the modulus, hardness and tension set increase with increase in PPA content. However, tensile strength, tear

TABLE III Physical properties at 25 °C

	Blend number							
Properties	B0	B1	B2	B3	B4	B5	B6	B7
Modulus at 50% elongation (MPa)	1.6	4.2	8.5	7.1	—	—	—	1.2
Modulus at 200% elongation (MPa)	2.0	9.0	12.4	—	—	—	—	2.8
Tensile strength (MPa)	13.0	34.5	22.6	8.0	8.8	11.7	16.9	3.1
Elongation at break (%)	852	630	400	106	30	10	5	480
Tear strength (kN m^{-1})	48.5	84.5	100.2	53.0	46.9	56.2	60.4	26.5
Hardness (shore A)	55	67	78	82	85	87	90	50
Tension set at 100% elongation (%)	7	10	25	30	—	—	—	33

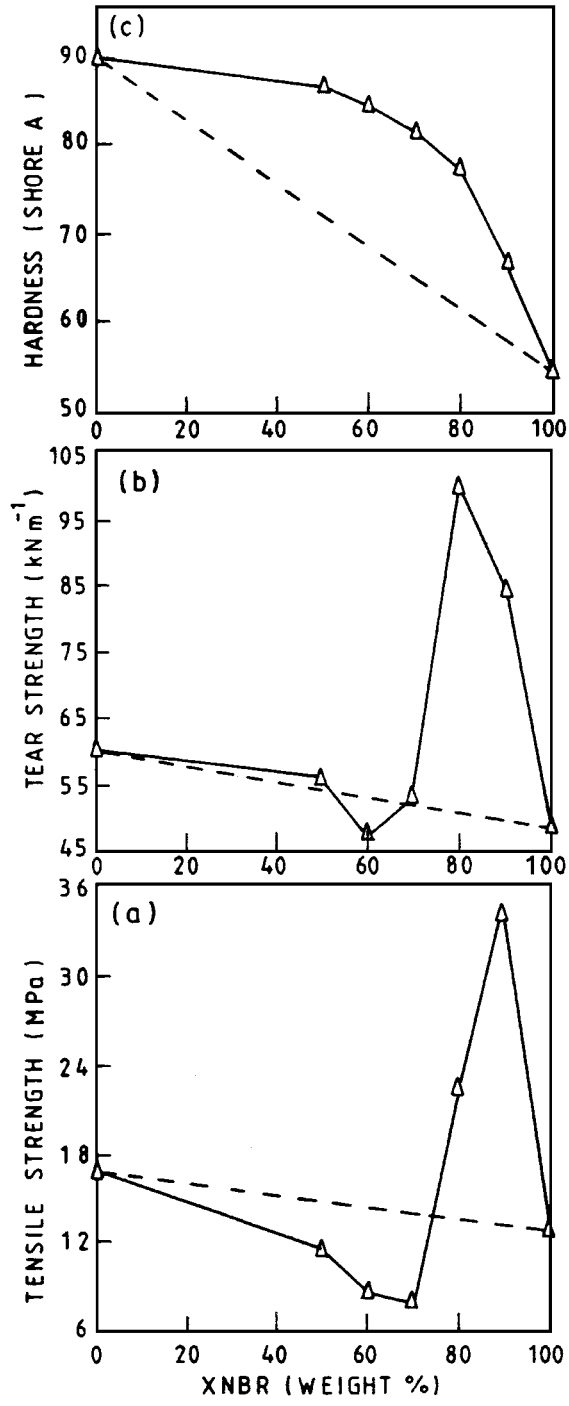

Figure 1 Variation of (a) tensile strength, (b) tear strength, (c) hardness with blend composition, △, observed values at 25 °C; -----, additivity line.

strength and elongation at break decrease sharply beyond 20% of PPA in the blends. It is also interesting to note that blends of Zn-XNBR and Zn-PPA show synergism in tensile strength and tear strength in the compositions of 90/10 and 80/20, parts by weight. Furthermore, hardness shows synergism in all blend compositions studied. It is also evident that the 80/20 Zn-XNBR/Zn-PPA composition (blend B2) exhibits higher physical properties than the corresponding non-ionomeric blend of 80/20 XNBR/PPA (blend B7). This is believed to be due to the interfacial ionic crosslinks, which enhance the compatibility by improving the interfacial adhesion between the two component phases [19–23]. Fig. 2 shows the scanning electron photomicrographs

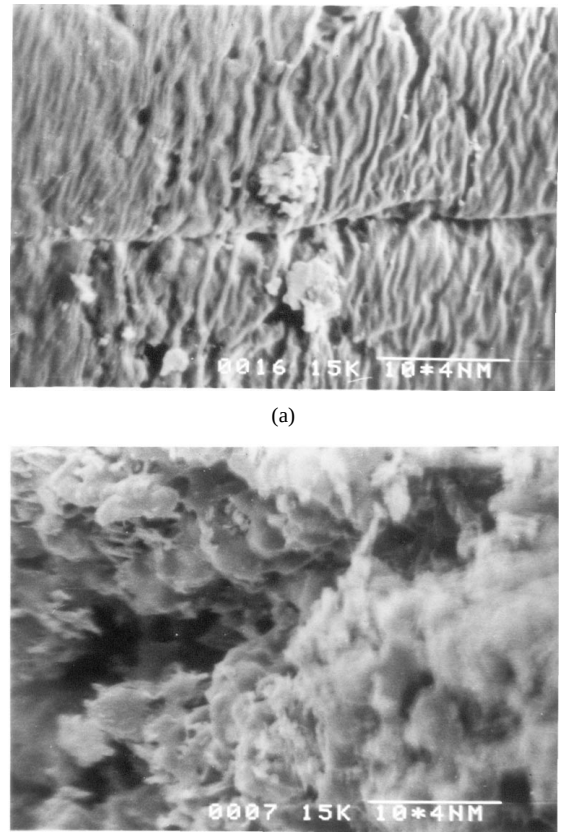

Figure 2 Scanning electron photomicrograph of the tear fractured surfaces of (a) blend B2 (b) blend B7.

of the tear fractured surfaces of blend B2 and blend B7. The fractogragh of blend B7 shows a straight tear path which propagated from one end to the other end, indicating poor tear resistance. On the other hand, the fractograph of blend B2 shows tear path with multiple deviations, indicating greater energy required for tearing. The ionic domains present in the blend B2 act as tear deviators and thereby enhances the tear resistance. The higher hardness and lower tension set of blend B2 is also the consequence of presence of ionic aggregates, which play the role of reinforcing filler and also act as physical crosslinks and thereby minimizes the set properties.

3.2. Infrared spectroscopic studies

The infrared spectra of the neat ionomers, (Zn-XNBR and Zn-PPA) are shown in Fig. 3. The spectrum of Zn-XNBR shows a weak band at 1666 cm^{-1}, which is indicative of the —C=C— stretching mode [25, 26]. The asymmetric carboxylate stretching region of the spectrum shows a doublet at 1591 and 1538 cm^{-1} [25, 27]. The splitting of COO^- stretching vibration is believed to be due to the existence of different co-ordinated structure of zinc cation [28, 29]. The band at 1591 cm^{-1} is assigned to the tetrahedral zinc carboxylate stretching, whereas the band at 1538 cm^{-1} may be due to the octahedral zinc carboxylate stretching [28, 29]. The band at 1591 cm^{-1} is strong and intense as compared to the band at 1538 cm^{-1}. The band at 1438 cm^{-1} is the characteristic of various —C—H vibrations [26]. The band at 1415 cm^{-1} denotes the symmetric carboxylate stretching and a weak band at 1355 cm^{-1} indicates the —CH_2—

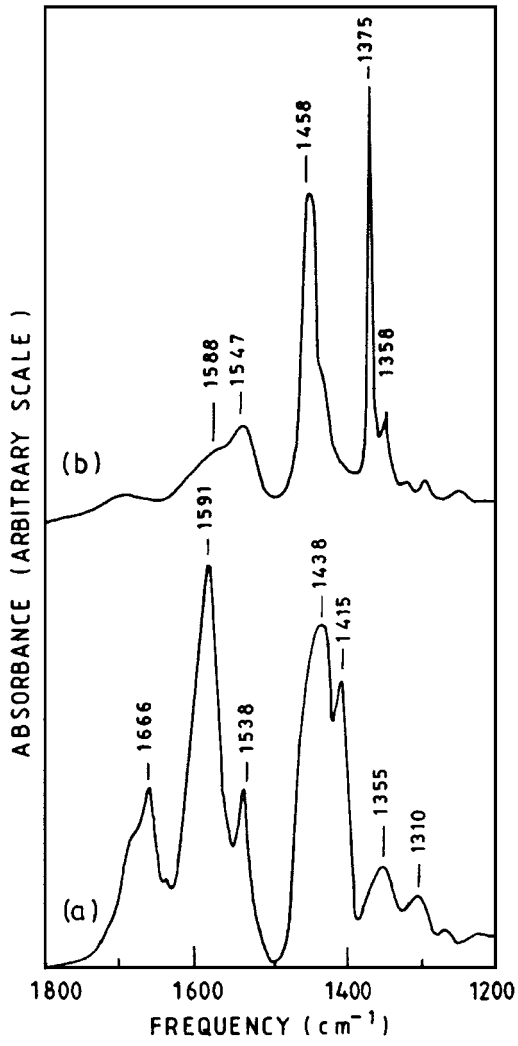

Figure 3 Infrared spectra of (a) Zn-XNBR and (b) Zn-PPA in the range of 1800–1200 cm^{-1}.

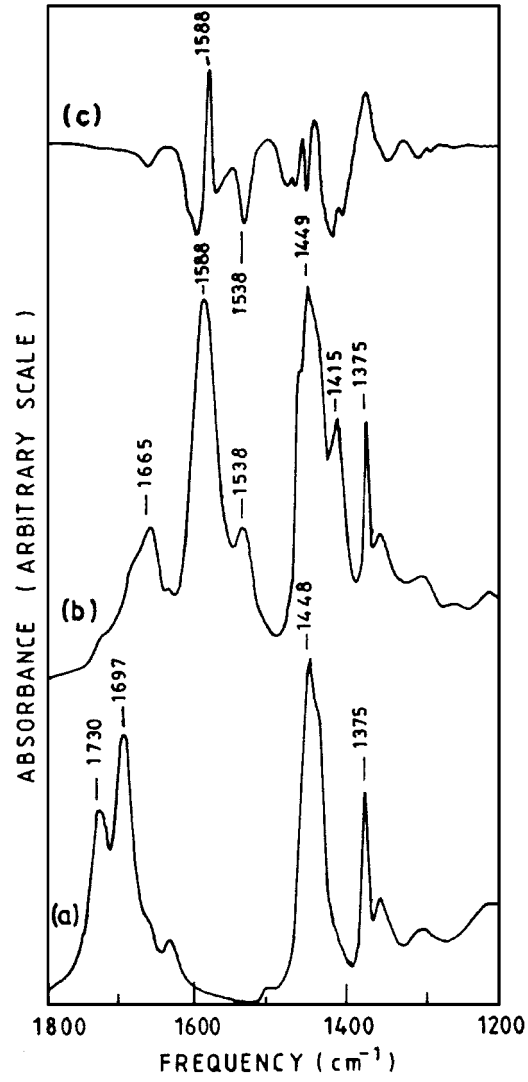

Figure 4 Infrared spectra of (a) blend B7, (b) blend B2 and (c) difference spectrum in the range of 1800–1200 cm^{-1}.

wagging vibration [25, 26]. The spectrum of Zn-PPA shows a broad band with a peak at 1547 cm^{-1} and a shoulder band at 1588 cm^{-1}, indicating the asymmetric metal carboxylate stretching. The strong band observed at 1458 cm^{-1} may be due to the coupled vibration of $-CH_2-$ bending and $-CH_3$ asymmetric deformation. An intense and sharp band at 1375 cm^{-1} is ascribed to the $-CH_3$ symmetric deformation [24, 25].

Fig. 4 shows the infrared spectra of the 80/20 non-ionomeric polyblend (blend B7) and the corresponding 80/20 ionomeric polyblend (blend B2). The spectrum of B7 shows a doublet at 1730 and 1697 cm^{-1} indicating the presence of carboxylic acid groups. The band at 1730 cm^{-1} is attributed to the presence of free carboxylic acid groups and the band at 1697 cm^{-1} accounts for the hydrogen bonded carboxylic acid pairs [25, 27]. The band at 1697 cm^{-1} may also be coupled with $-C{=}C-$ stretching. The strong band at 1448 cm^{-1} is associated with the coupled vibration of $-CH_2-$ bending and $-CH_3$ asymmetric deformation. The sharp band at 1375 cm^{-1} is assigned to the $-CH_3$ symmetric deformation. There exists a marked difference between the spectra of blend B7 and blend B2. It is seen that instead of a doublet at 1730 and 1697 cm^{-1} in the case of blend B7, the spectrum of blend B2 shows a doublet at 1588 and 1538 cm^{-1}. The bands at 1588 and 1538 cm^{-1} as explained earlier, indicate the metal carboxylate stretching vibration [25, 27]. A weak band at 1415 cm^{-1} denotes the symmetric metal carboxylate vibration. Appearence of these bands in blend B2 indicate the formation of metal carboxylate ions by the neutralization of carboxylic acid groups, present in blend B7. Fig. 3c shows the difference spectrum. The difference spectrum was obtained by substracting the summation spectrum (that is, weighted addition of the spectra of the neat ionomers) from blend B2. It is seen that the difference spectrum shows a positive absorption at 1588 cm^{-1} and a negative absorption at 1536 cm^{-1}. This is indicative of the changes in spectral profile in the blend, due to the intermolecular interaction of zinc carboxylate ions in the neat ionomers.

3.3. Dynamic mechanical thermal analysis

Fig. 5 shows the plots of tan δ versus temperature of the neat ionomers and the ionomeric polyblends. The results of dynamic mechanical thermal analyses are given in Table IV. It can be seen that Zn-XNBR shows a main glass-rubber transition (T_g) at 4 °C and another transition at 50 °C. The high temperature transition is attributed to the presence of ionic clusters in Zn-XNBR.

TABLE IV Results of dynamic mechanical thermal analyses

Blend number	T_g (°C)	tan δ at T_g	T_i (°C)	tan δ at T_i
B0	4	0.531	50	0.357
B1	8	0.465	50	0.322
B2	10	0.390	56	0.270
B3	5	0.317	57	0.212
B4	4	0.210	72	0.162
B5	5	0.177	70	0.156
B6	9	0.067	75	0.104
B7	−1	0.510	—	—

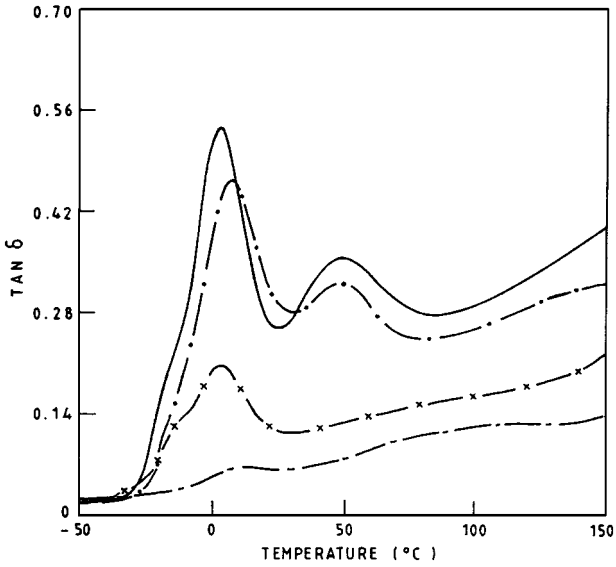

Figure 5 Plots of tan δ versus temperature of Zn-XNBR (—); Zn-PPA (– - –); blend B1 (— • —); and blend B4 (– × –).

The temperature corresponds to the high temperature transition is hereafter abbreviated as T_i. It is known that in the case of ion-containing polymers ion-pairs segregate to form a separate rigid phase, which contains restricted mobility segments of the polymer chains along with the ionic aggregates [30, 31]. The high temperature transition is due to the relaxation of the segments of the restricted mobility polymer chains in the ionic cluster region [31]. Zn-mPP shows a glass-rubber transition at 9 °C and the high temperature transition at 75 °C. The T_g values of the neat polymers are very close, and therefore, the criterion of a single composition-dependent T_g could not be used to assess the miscibility of the blends [16]. There occurs a marginal increase in the T_g of Zn-XNBR with the addition of PPA upto 20 parts, after that there occurs insignificant changes in the T_g values. As expected, the tan δ at T_g of the blends decreases with increase in PPA content in the blend. This is attributed to the decrease in amorphous Zn-XNBR phase in the blend, as well as due to the ionic interactions, which increase the stiffness of the blends. As observed in the case of neat ionomers, the ionomeric polyblends also exhibit a high temperature transition. The T_i value of the blends slightly increase with increase in PPA content. However, the tan δ at T_i decrease with increase in PPA content. Furthermore, it is also seen that the high temperature transition is broadened with increase in PPA content.

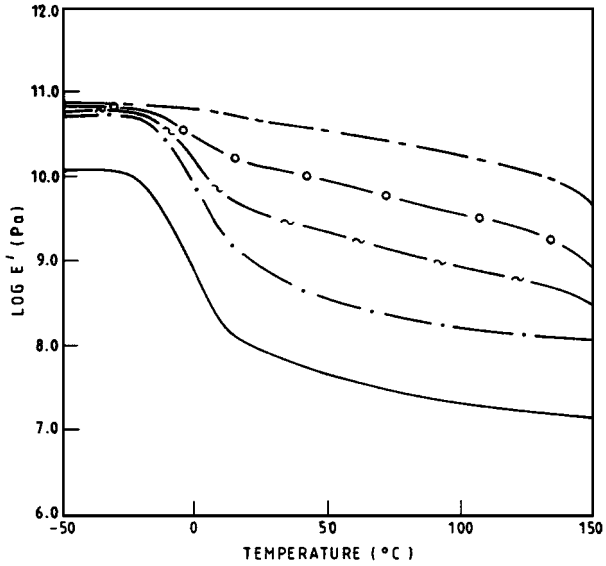

Figure 6 Plots of log E' versus temperature of Zn-XNBR (—); Zn-PPA (– - –); blend B1 (— • —); blend B3 (– ~ –) and blend B5 (– ○ –).

Fig. 6 shows the plot of log E' versus temperature of the neat ionomers and the ionomeric polyblends. Zn-mPP shows relatively high modulus due to its crystallinity, whereas Zn-XNBR shows relatively low modulus owing to its amorphous nature. The existence of a rubbery plateau over a wide temperature span is believed to be due to the presence of ionic crosslinks in Zn-XNBR. As expected the modulus of the blends increase with increase in PPA content. Fig. 7 shows the variation of log E' with blend composition at 30, 70 and 100 °C. It is interesting to note that, as observed in the case of hardness, the blends show synergism in storage modulus at all temperatures. This may be due to the reinforcing ability of the ionic domains present in the blends [4].

Finally, in order to confirm the role of ionic aggregates on the reinforcing ability and the high temperature transition, we have studied the dynamic mechanical properties of blend B2 and the corresponding non-ionomeric polyblend (that is, blend B7). Fig. 8 shows the plot of tan δ and log E' versus temperature of blend B2 and blend B7. It is interesting to note that blend B2 exhibits higher modulus at all temperatures than blend B7. It is also seen that tan δ at T_g of blend B2 is much less than blend B7. This is attributed to the presence of intermolecular ionic interactions, which increase the stiffness and also slightly increases the T_g of blend B2. Furthermore, the ionomeric polyblend shows a high temperature transition at 56 °C, owing to the relaxation of the restricted mobility polymer chains in the ionic cluster region, whereas the same is absent in the corresponding non-ionomeric polyblend.

3.4. Processability studies

Fig. 9 shows the log-log plot of apparent viscosity versus temperature of the ionomeric polyblend (blend B2) and the corresponding non-ionomeric polyblend (blend B7). It is apparent that blend B2 shows higher melt viscosity than blend B7. The higher melt viscosity of the ionomeric polyblend is presumably due to the

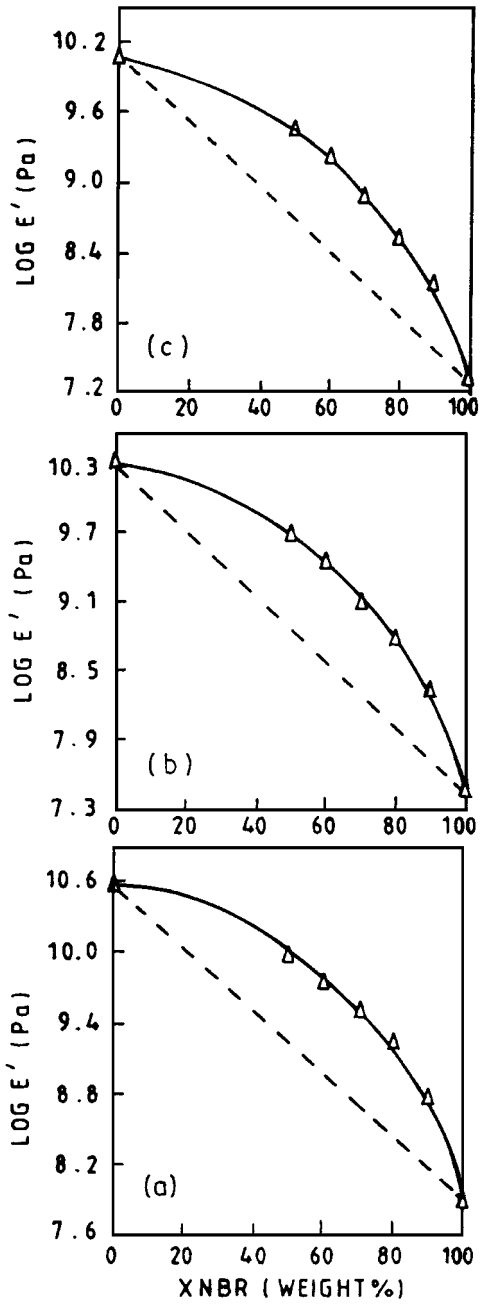

Figure 7 Variation of log E' at (a) 30 °C, (b) 70 °C and (c) 100 °C with blend composition △, observed values; ----, additivity line.

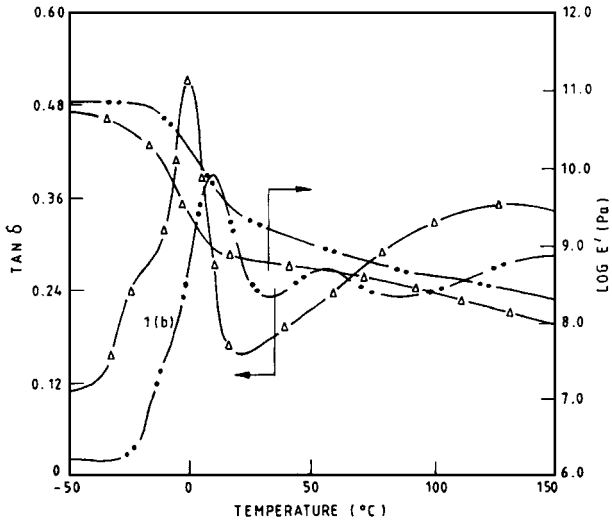

Figure 8 Plots of $\tan\delta$ and $\log E'$ versus temperature for blend B2 (–●●–) and blend B7 (–△–).

TABLE V Results of X-ray studies

Property	Blend number							
	B1	B2	B3	B4	B5	B6	B7	PPA
Percent crystalinity (%)	3	8	14	18	25	43	12	52

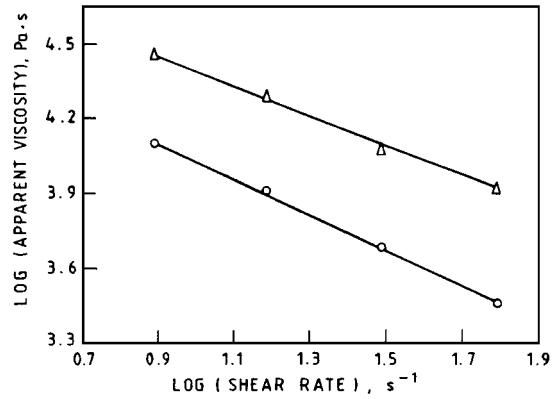

Figure 9 Log-log plots of apparent viscosity versus shear rate at 230 °C of blend B2 (△) and blend B7 (○).

occurrence of ionic crosslinks in the polymer chains which resist the melt flow. The apparent viscosity of the blends decreases with increasing shear rate, indicating the pseudoplastic nature of the blends.

3.5. X-ray studies

Results of X-ray studies are given in Table V. It is known that ionomer formation decreases the crystallinity of the polymer [4]. It is seen that ionomer formation causes reduction in crystallinity of PPA and blend B7. It is also evident that blends B1 and B2 exhibit low crystallinity. It is inferred that crystallinity has no role to play in the properties of blends.

3.6. Scanning electron microscopic studies

Fig. 10 shows the scanning electron photomicrographs of the ionomeric polyblend (blend B2) and the corresponding non-ionomeric polyblend (blend B7). It is apparent that blend B2 is compatible, as indicated by the homogeneity of the two phases with interpenetrating type network, whereas the blend B7 is grossly incompatible, as indicated by the heterogeneity of the two phases and roughness of the fracture surface.

3.7. Reprocessability studies

Results of reprocessability studies of the 80/20 Zn-XNBR/Zn-PPA blend (blend B2) obtained by repeated melting and moulding is given in Table VI. It is

TABLE VI Results of reprocessability studies of blend B2 at 200 °C

Number of cycles	Tensile strength (MPa)	Modulus at 200% (MPa)	Elongation at break (%)
1	22.6	12.4	400
2	20.1	12.8	380
3	21.3	13.2	385

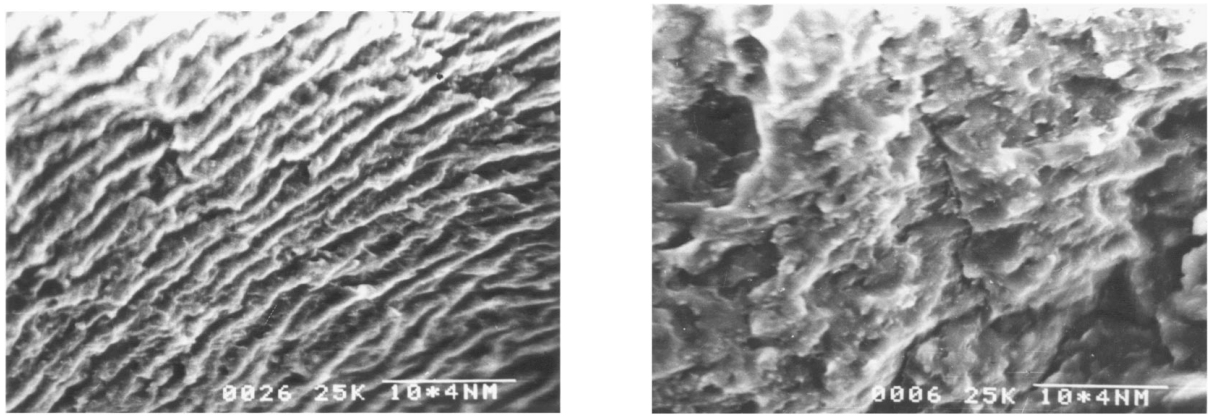

(a) (b)

Figure 10 Scanning electron photomicrographs of (a) blend B2 and (b) blend B7.

apparent that the modulus, tensile strength and elongation at break of the blend remain constant, even after three cycle of melting and moulding. This is indicative of the thermal stability as well as the thermoplastic elastomeric nature of the blends. The reprocessability of the blend is believed to be due to the thermolabile nature of the ionic and crystalline domains in the blend.

Fig. 11 shows the schematic representation of formation of an ionic cluster in the ionomeric polyblend. The carboxylic acid groups present in the polymers are neutralized by zinc oxide in presence of stearic acid, which results in zinc carboxylate ions. The ionic groups anchor the polymer chains in their vicinity and form a restricted mobility region.

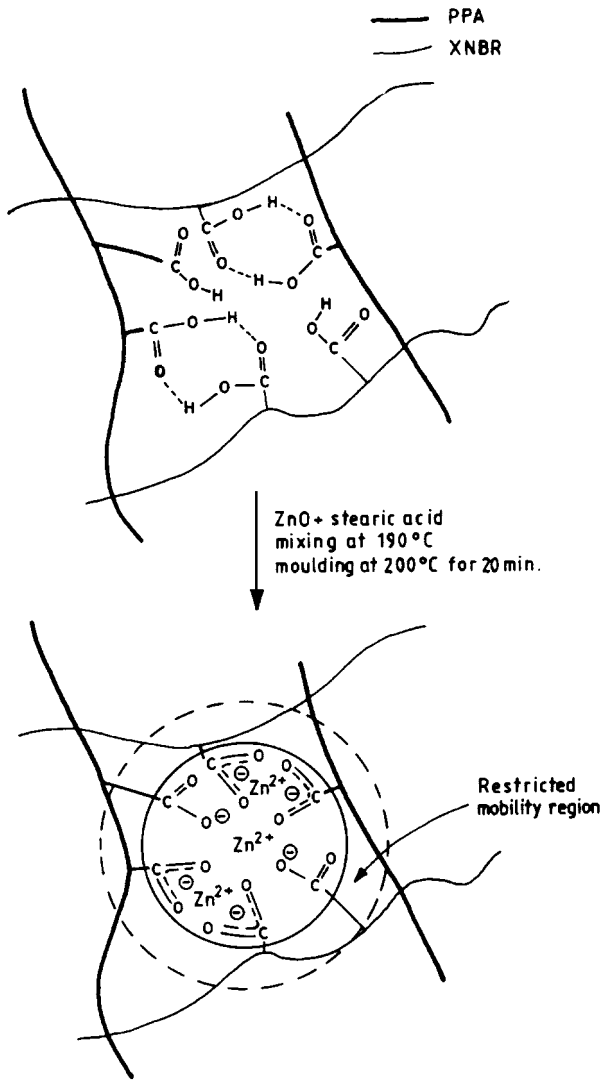

Figure 11 Schematic representation of formation of ionic cluster in the Zn-XNBR/Zn-PPA blend.

4. Conclusions

The ionomeric polyblends of Zn-XNBR and Zn-PPA in the compositions of 90/10 and 80/20, parts by weight, behave as ionic thermoplastic elastomers, with synergism in physical properties. Infrared spectroscopic studies reveal the formation of the ionomer as well as the intermolecular ionic interactions in the blend. The biphasic nature of the ionomeric polyblends is evident from the dynamic mechanical thermal analyses, which show an additional relaxation at high temperature due to the presence of ionic domains. The ionomeric polyblend shows higher physical properties and melt viscosity than the corresponding non-ionomeric polyblend.

References

1. L. HOLLIDAY (Ed.), "Ionic polymers" (Applied Science, London, 1975).
2. A. EISENBERG and M. KING, "Ion-containing Polymers: Physical Properties and Structure" (Academic Press, New York, 1977).
3. W. J. MACKNIGHT and T. R. EARNEST, *J. Polym. Sci. Macromol. Rev.* **16** (1981) 41.
4. C. G. BAZUIN and A. EISENBERG, *Ind. Eng. Chem. Prod. Res. Dev.* **20** (1981) 271.
5. W. J. MACKNIGHT and R. D. LUNDBERG, *Rubber Chem. Technol.* **57** (1984) 652.
6. *Idem.*, in "Thermoplastic Elastomers," edited by N. R. Legge, G. Holden and H. E. Schroeder (Hanser, Munich, 1987) p. 245.
7. J. J. FITZGERALD and R. A. WEISS, *J. Macromol. Sci. Chem. Rev. Macromol. Chem. Phys.* **28**(1) (1988) 99.
8. M. M. COLEMAN, J. F. GRAF and P. C. PAINTER, "Specific Interactions and the Miscibility of Polymer Blends" (Technomic Publishing Co., USA, 1991).
9. O. OLABISI, L. M. ROBESON and M. T. SHAW, "Polymer-Polymer Miscibility" (Academic Press, New York, 1979).
10. Z. L. ZHOU and A. EISENBERG, *J. Polym. Sci., Polym. Phys. Ed.* **21** (1983) 595.
11. M. RUTKOWSKA and A. EISENBERG, *J. Appl. Polym. Sci.* **29** (1984) 755.

12. M. HARA and A. EISENBERG, *Macromolecules* **17** (1984) 1335.
13. M. RUTKOWSKA and A. EISENBERG, *ibid*. **17** (1984) 821.
14. *Idem., J. Appl. Polym. Sci*. **30** (1985) 2317.
15. X. LU and R. A. WEISS, *Macromolecules* **24** (1991) 4381.
16. E. P. DOUGLAS, K. SAKURAI and W. J. MACKNIGHT, *ibid.* **24** (1991) 6776.
17. X. LU and R. A. WEISS, *ibid*. **25** (1992) 6185.
18. Y. KIM, W. J. CHO and C. S. HA, *Polym. Eng. Sci.* **35** (1995) 1592.
19. T. KURIAN, S. DATTA, D. KHASTGIR, P. P. DE, D. K. TRIPATHY, S. K. DE and D. G. PEIFFER, *Polymer* **37** (1996) 4787.
20. S. DATTA, P. P. DE and S. K. DE, *J. Appl. Polym. Sci*. **61** (1996) 1839.
21. P. ANTONY and S. K. DE, *Plas. Rubber Compos. Process. Appl*. **26** (1997) 311.
22. *Idem., J. Appl. Polym. Sci*. **70** (1998) 483.
23. *Idem., Polymer* **40** (1999) 1487.
24. S. DATTA, S. K. DE, E. G. KONTOS and J. M. WEFER, *J. Appl. Polym. Sci.* **61** (1996) 177.
25. S. L. SMITH, "Applied Infrared Spectroscopy" (Wiley Interscience Publication, New York, 1979) p. 287.
26. M. M. COLEMAN and P. C. PAINTER, *J. Macromol. Sci. Rev. Macromol. Chem*. **C16**(2) (1977) 1971.
27. D. H. WILLIAMS and I. FLEMING, "Spectroscopic Methods in Organic Chemistry" (McGraw-Hill, London, 1987).
28. B. A. BROZOSKI, M. M. COLEMAN and P. C. PAINTER, *Macromolecules* **17** (1984) 230.
29. M. M. COLEMAN, J. Y. LEE and P. C. PAINTER, *ibid.* **23** (1990) 2339.
30. A. EISENBERG, B. HIRD and R. B. MOORE, *ibid.* **23** (1990) 4098.
31. B. HIRD and A. EISENBERG, *ibid.* **25** (1992) 6466.

Received 27 July
and accepted 12 November 1998